

Novel Optical and Magnetic Bistability and Photoinduced Transition in a One-Dimensional Halogen-Bridged Binuclear Pt Complex

H. Matsuzaki,¹ T. Matsuoka,¹ H. Kishida,¹ K. Takizawa,² H. Miyasaka,² K. Sugiura,²
M. Yamashita,² and H. Okamoto^{1,3,*}

¹Department of Advanced Materials Science, University of Tokyo, Kashiwa, Chiba, 277-8561, Japan

²Department of Chemistry, Tokyo Metropolitan University, Hachioji, Tokyo, 192-0397, Japan

³Correlated Electron Research Center (CERC), National Institute of Advanced Industrial Science and Technology (AIST), Tsukuba, 305-0046, Japan

(Received 18 July 2002; published 28 January 2003)

In iodine-bridged binuclear Pt compounds, $R_4[\text{Pt}_2(\text{pop})_4\text{I}]n\text{H}_2\text{O}$ and $R'_2[\text{Pt}_2(\text{pop})_4\text{I}]n\text{H}_2\text{O}$ ($\text{pop} = \text{P}_2\text{O}_5\text{H}_2^-$), electronic structures on the PtI chains have been controlled between a diamagnetic charge-density-wave (CDW) state and a paramagnetic charge-polarization (CP) state by modification of the counterions (R, R') located between chains. In the $R = (\text{C}_2\text{H}_5)_2\text{NH}_2^+$ compound, a pressure-induced CP to CDW transition with a drastic color change is identified. This transition is accompanied by a large hysteresis loop within which photoinduced transition between CDW and CP can be driven by selecting the excitation photon energy.

DOI: 10.1103/PhysRevLett.90.046401

PACS numbers: 71.30.+h, 71.45.Lr, 78.30.Hv, 78.40.Ha

The control of phase transitions and related macroscopic properties by photoirradiation has recently attracted much attention [1–6]. This phenomenon is called photoinduced phase transition (PIPT) and is important not only as a new phenomenon in the fields of physics and chemistry, but also as a useful mechanism applicable to future optical switching devices. A key strategy toward realizing PIPT is the exploration of one-dimensional (1D) materials. The 1D electronic states essentially include strong instabilities inherent to electron-lattice and/or electron-electron interactions and sometimes produce characteristic phase transitions at low temperature. PIPTs have been driven in a π -conjugated polymer, polydiacetylene (PDA) [2], and an organic charge transfer (CT) complex, tetrathiafulvalene-*p*-chloranil (TTF-CA) [1,6] by the irradiation of light near the phase transition temperature. PIPTs in 1D systems are, however, limited to these organic materials. No PIPTs have been found in 1D transition metal complexes and other 1D inorganic materials. Moreover, PDA and TTF-CA are always diamagnetic, and magnetic properties do not change appreciably in their PIPTs. Here we report a PIPT in a halogen-bridged binuclear-metal compound with a drastic change in both optical and magnetic properties. This compound has a purely 1D chain composed of repeating metal-metal-halogen (M - M - X) units with $M = \text{Pt}$ and $X = \text{I}$, called a MMX chain.

In the MMX chain, a 1D electronic state is formed by d_z orbitals of M and p_z orbitals of X . The average valence of M is 2.5, and 3 electrons exist per two d_z orbitals. Four charge-ordering (CO) states are theoretically expected in this system [7–9]; average valence state ($X-M^{2.5+}-M^{2.5+}-X$), charge-density-wave (CDW) state ($X-M^{2+}-M^{2+}-X-M^{3+}-M^{3+}-X$), charge-polarization (CP) state ($X-M^{2+}-M^{3+}-X-M^{2+}-M^{3+}-X$), and alter-

nating charge-polarization (ACP) state ($X-M^{2+}-M^{3+}-X-M^{3+}-M^{2+}-X$). CDW and CP are stabilized by the displacements of X , while ACP is stabilized by the displacements of M dimers. Two classes of MMX chains with different ligand molecules, $R_4[\text{Pt}_2(\text{pop})_4X]n\text{H}_2\text{O}$ ($R = \text{K}^+, \text{NH}_4^+$, and $X = \text{Cl}^-, \text{Br}^-$) [10,11] and $\text{Pt}_2(\text{dta})_4\text{I}$ ($\text{dta} = \text{CH}_3\text{CS}^-$) [12,13] have been studied thus far. The ground state of the former was revealed to be CDW [14]. For the latter, it has been suggested that ACP is stabilized at low temperature [13], but their electronic states have not been fully clarified yet. As a general trend, hybridization between the p orbital of X and the d orbital of M in the I-bridged compounds is larger than that in the Cl- or Br-bridged compounds. The large pd hybridization will stabilize the various CO states. In our study, therefore, we focus on the I-bridged compounds with pop for the ligands.

We have synthesized about 20 compounds of $R_4[\text{Pt}_2(\text{pop})_4\text{I}]n\text{H}_2\text{O}$ and $R'_2[\text{Pt}_2(\text{pop})_4\text{I}]n\text{H}_2\text{O}$, with counterions of the alkyl-ammonium [$R = \text{C}_n\text{H}_{2n+1}\text{NH}_3^+$, $(\text{C}_n\text{H}_{2n+1})_2\text{NH}_2^+$, and $R' = \text{H}_3\text{N}(\text{C}_n\text{H}_{2n})\text{NH}_3^+$] and the alkali metal ($R = \text{Na}^+, \text{NH}_4^+, \text{Rb}^+, \text{and Cs}^+$). The substitution of the counterions greatly alters the distance $d(\text{Pt-I-Pt})$ between the two Pt ions bridged by the I ion. Such control of $d(\text{Pt-I-Pt})$ makes it possible to realize the paramagnetic CP state as well as the diamagnetic CDW state. Moreover, the transitions between these two CO states can be induced by applying pressure. In $[(\text{C}_2\text{H}_5)_2\text{NH}_2]_4[\text{Pt}_2(\text{pop})_4\text{I}]$, the pressure-induced phase transition (PRIPT) from CP to CDW is accompanied by a large hysteresis loop. We have found a PIPT between the two CO states within this loop.

Single crystals of the MMX chains were synthesized by a modification of the method in [15]. X-ray structural analysis was performed using an imaging plate

diffractometer. Reflectivity spectra were obtained using a specially designed monochromator and a Fourier transform infrared spectrometer, equipped with optical microscopes. The obtained reflectivity spectra were converted to optical conductivity using the Kramers-Kronig transformation. Raman spectra were measured using a Raman spectrometer equipped with an Ar ion laser, a He-Ne laser, and an optical microscope. Measurements under pressure were performed using a diamond anvil cell. Liquid paraffin was used as a pressure medium. Spin susceptibility χ_{spin} was measured using a SQUID magnetometer and an electron spin resonance spectrometer.

Figure 1(a) shows the structure of $[(\text{C}_2\text{H}_5)_2\text{NH}_2]_4[\text{Pt}_2(\text{pop})_4\text{I}]$. Two Pt ions are linked by four pop molecules, forming a binuclear $\text{Pt}_2(\text{pop})_4$ unit. The two neighboring $\text{Pt}_2(\text{pop})_4$ units are bridged by I, and the PtPtI chain structure is formed along the c axis. The I ion deviates from the midpoints between the two neighboring Pt ions, indicating that this compound is in CDW or CP, as illustrated in Fig. 1(b). Figure 1(a) shows the two possible positions of I, as the displacements of I are not three-dimensionally ordered. X-ray structural analysis was unable to resolve whether the ground state is CDW or CP. CP is composed of $\text{Pt}^{2+}\text{-Pt}^{3+}$ units, and the Pt^{3+} ions have spin ($S = 1/2$), forming a 1D antiferromagnetic spin chain. CDW, on the other hand, is composed of $\text{Pt}^{2+}\text{-Pt}^{2+}$ and $\text{Pt}^{3+}\text{-Pt}^{3+}$ units and is diamagnetic because the two neighboring Pt^{3+} ions form a singlet state. The ground states of the PtPtI chains can then be discussed, keeping these characteristics of the two CO states in mind.

Figure 2(a) shows the optical conductivity spectra of $[(\text{C}_2\text{H}_5)_2\text{NH}_2]_4[\text{Pt}_2(\text{pop})_4\text{I}]$ (the material A) and $[\text{H}_3\text{N}(\text{C}_6\text{H}_{12})\text{NH}_3]_2[\text{Pt}_2(\text{pop})_4\text{I}]$ (the material B) as typical examples. The optical gap energies E_{CT} (1.0 and 2.4 eV)

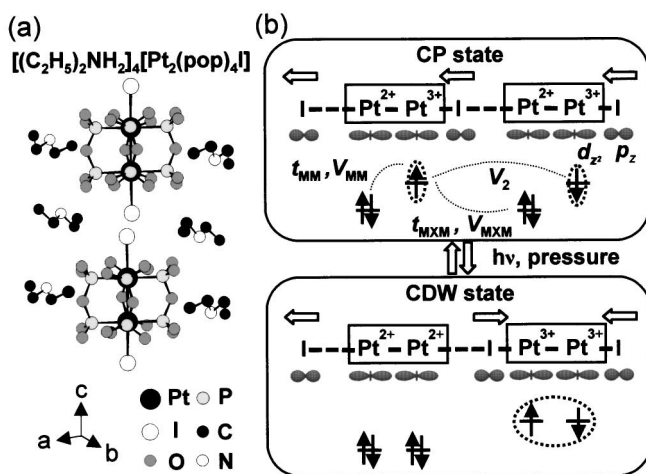


FIG. 1. (a) Crystal structure of $[(\text{C}_2\text{H}_5)_2\text{NH}_2]_4[\text{Pt}_2(\text{pop})_4\text{I}]$. H atoms have been omitted for clarity. (b) Schematic electronic structures of CDW and CP. t_{MM} and t_{MXM} denote the electron transfer energies. V_{MM} , V_{MXM} , and V_2 denote the Coulomb interactions.

046401-2

of the two compounds differ considerably. The Raman spectra are shown in the inset to provide information concerning the valence of M [10,13]. Strong bands at $80\text{--}100\text{ cm}^{-1}$ are attributed to the Pt-Pt stretching mode of the Pt-Pt unit. The splitting of this mode indicates the formation of two kinds of Pt-Pt units, in this case $\text{Pt}^{2+}\text{-Pt}^{2+}$ and $\text{Pt}^{3+}\text{-Pt}^{3+}$. The ground state of B can therefore be considered to be CDW. In A , this Pt-Pt stretching mode is a single band, suggesting that the ground state is CP. The weak bands around 110 cm^{-1} can be attributed to the Pt-I stretching mode, which is activated by the displacements of I in both compounds.

The magnetic properties of the materials were then investigated to confirm these assignments. The temperature dependence of χ_{spin} ($1/\chi_{\text{spin}}$) is presented in Fig. 2(b). In B , χ_{spin} follows the Curie law as shown by the broken line in Fig. 2(b) (the upper figure). Curie impurities make up 0.16% per Pt site. No paramagnetic components originate from the 1D spin chains. In A , on the other hand, the temperature dependence of χ_{spin} cannot be explained by the Curie component alone. There is a finite component independent of temperature, attributed to a contribution from the 1D spin chain. The Bonner-Fisher (BF) curve, applicable to a 1D antiferromagnetic $S = 1/2$ chain, shows that χ_{spin} is only slightly dependent on temperature when the exchange interaction J is much larger than 300 K. The result in Fig. 2(b) (the lower figure) can be largely reproduced by the sum of the BF curve with $J \sim 3000$ K and Curie component with the concentration of 0.34% per Pt site. From these comparative studies, we

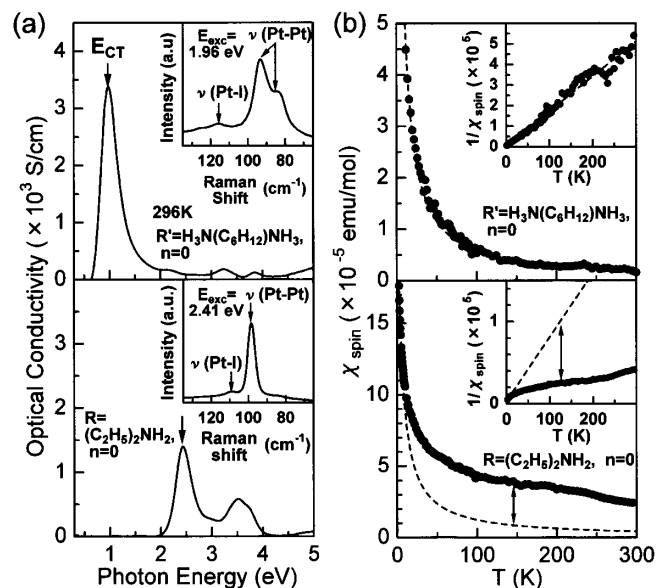


FIG. 2. (a) Optical conductivity spectra with light polarization parallel to the chain axis in $[(\text{C}_2\text{H}_5)_2\text{NH}_2]_4[\text{Pt}_2(\text{pop})_4\text{I}]$ (the material A) and $[\text{H}_3\text{N}(\text{C}_6\text{H}_{12})\text{NH}_3]_2[\text{Pt}_2(\text{pop})_4\text{I}]$ (the material B), and Raman spectra (inset) for polarization of $z(xx)\bar{z}$ ($x \parallel$ chain axis). (b) Temperature dependence of χ_{spin} and $1/\chi_{\text{spin}}$ (inset). Broken lines represent Curie components.

046401-2

can conclude that the ground states of A and B are CP and CDW, respectively.

The phase diagram shown in Fig. 3 was compiled based on systematic optical, magnetic, and x-ray studies on PtPtI chains with different counterions. The upper figure represents the magnitude of the splitting in the Pt-Pt stretching Raman band $\Delta\nu(\text{Pt-Pt})$, evidence of CDW. The lower figure shows the optical gap energy E_{CT} . The ground state changes from CP to CDW with decreasing $d(\text{Pt-I-Pt})$, and there is a clear boundary at around 6.1 Å.

Here let us briefly discuss the stability of CP and CDW as a function of $d(\text{Pt-I-Pt})$, taking account of the theoretical studies based on the one-band extended Peierls-Hubbard model [8,16]. When $d(\text{Pt-I-Pt})$ is large, the intradimer Coulomb interaction V_{MM} and the intradimer transfer energy t_{MM} are important parameters dominating the ground state in addition to the on-site Coulomb repulsion U_M on M and the site-diagonal-type electron-lattice interaction β . The interdimer interactions such as the transfer energy t_{MXM} , the Coulomb interaction V_{MXM} , and the second nearest neighbor Coulomb interaction V_2 [see Fig. 1(b)] can be neglected. A simple picture is given by considering the localized limit ($t_{MM} = 0$). In this case, the relative energy of CP and CDW is determined by V_{MM} . The sum of the Coulomb energy for two neighboring M dimers in CDW ($5V_{MM}$) is larger than that in CP ($4V_{MM}$). Therefore, V_{MM} stabilizes CP. Under the presence of t_{MM} , the bonding orbital in the M dimer is formed in CP, but not formed in CDW because of large U_M . As a result, t_{MM} also stabilizes CP. As $d(\text{Pt-I-Pt})$ decreases, V_{MXM} , V_2 , t_{MXM} , and β will increase. The increase of V_2 makes CP rather unstable, while V_{MXM} does not affect the relative

energy of CP and CDW. The effects of t_{MXM} and β are not so straightforward. The theoretical calculations have revealed that the increase of β and t_{MXM} also stabilize CDW relatively to CP [16]. Thus, the theoretical studies can explain well the experimental result that the ground state changes from CP to CDW with a decrease of $d(\text{Pt-I-Pt})$.

From the phase diagram in Fig. 3, it is expected that a phase transition can be driven by applying pressure to the materials in CP. Such a PRIPT from CP to CDW has indeed been observed for the material A , $[(\text{C}_5\text{H}_{11})_2\text{NH}_2]_4[\text{Pt}_2(\text{pop})_4\text{I}]$ and $[(\text{C}_3\text{H}_7)_2\text{NH}_2]_4[\text{Pt}_2(\text{pop})_4\text{I}]$. Photographs of the PRIPT in A are presented in Fig. 4(a). At ambient pressure, this material is green [Fig. 4(a)-(i)]. When the pressure is increased to 0.6 GPa, a brown region appears [Fig. 4(a)-(ii)] and grows gradually [Fig. 4(a)-(iii), (iv)]. Figure 4(b) shows the change in the Raman spectra accompanying this PRIPT. The Pt-Pt stretching band clearly splits at above 0.6 GPa, indicating that the high-pressure brown phase is CDW. Figure 4(c) shows the pressure dependence of E_{CT} , obtained from an analysis of the polarized reflectivity spectra. The transition is a first-order reversible one with a large hysteresis loop (ca. 0.4 GPa).

Images of the crystal reveal that the sample size along the chain axis c is reduced by ca. 8% at 0.85 GPa compared to ambient pressure. If the Pt-Pt distance $d(\text{Pt-Pt})$ of the Pt-Pt unit is assumed to remain constant under pressure, $d(\text{Pt-I-Pt})$ at 0.85 GPa is estimated 6.2 Å. This assumption is reasonable because $d(\text{Pt-Pt})$ is almost constant in various MMX chains. The obtained values, $d(\text{Pt-I-Pt}) = 6.2$ Å and $E_{\text{CT}} = 1.6$ eV at 0.85 GPa, are very close to those in CDW (see Fig. 3). That is, PRIPT from CP to CDW is driven by a decrease in $d(\text{Pt-I-Pt})$.

At points a and b in Fig. 4(c), the material is in a metastable state as shown in the energy potential curves (inset). The PIPT from the metastable state to the ground state at points a and b were investigated. Figure 4(d)-(i) shows the images of the sample at a before and after photoirradiation with 2.41-eV light for 8 ms. As can be seen, the crystal exhibits a permanent color change from brown to green in the irradiated region. The Raman signal in the irradiated region is almost identical to that of the low-pressure phase. To clarify whether this PIPT is induced by an optical process or laser heating, the dependence of the PIPT efficiency on the excitation photon density N was investigated for two excitation energies E_{ex} of 1.96 and 2.41 eV. N was calculated considering the absorption coefficient and the reflection loss of the excitation light, and the converted fractions were estimated from the photoinduced changes in the integrated intensity of the Pt-Pt stretching Raman bands. The PIPT efficiency exhibits a clear threshold N_{th} (photon density per 8 ms pulse), the values of which are strongly dependent on E_{ex} ($N_{\text{th}} \sim 1.4 \times 10^{25} \text{ cm}^{-3}$ at $E_{\text{ex}} = 1.96$ eV and $\sim 3 \times 10^{24} \text{ cm}^{-3}$ at 2.41 eV). This characteristic excitation energy dependence of N_{th} demonstrates that the observed PIPT is driven not by laser heating but by an optical

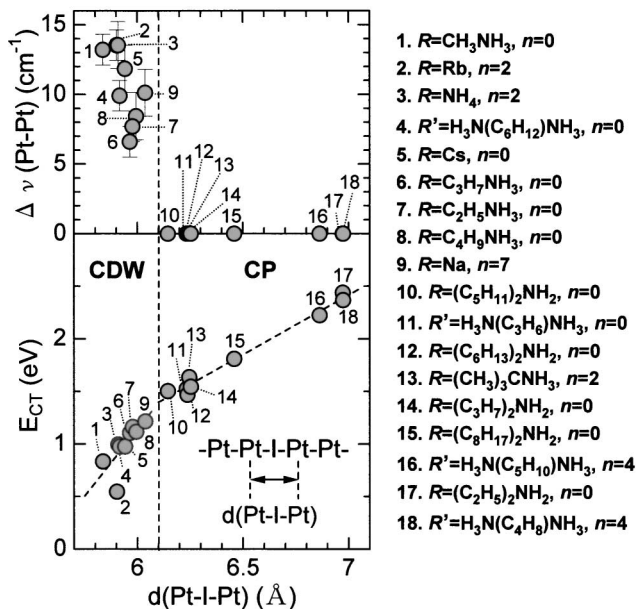


FIG. 3. The magnitude of the splitting in the Pt-Pt stretching Raman band $\Delta\nu(\text{Pt-Pt})$ and the optical gap energy E_{CT} as a function of $d(\text{Pt-I-Pt})$ in the MMX chains.

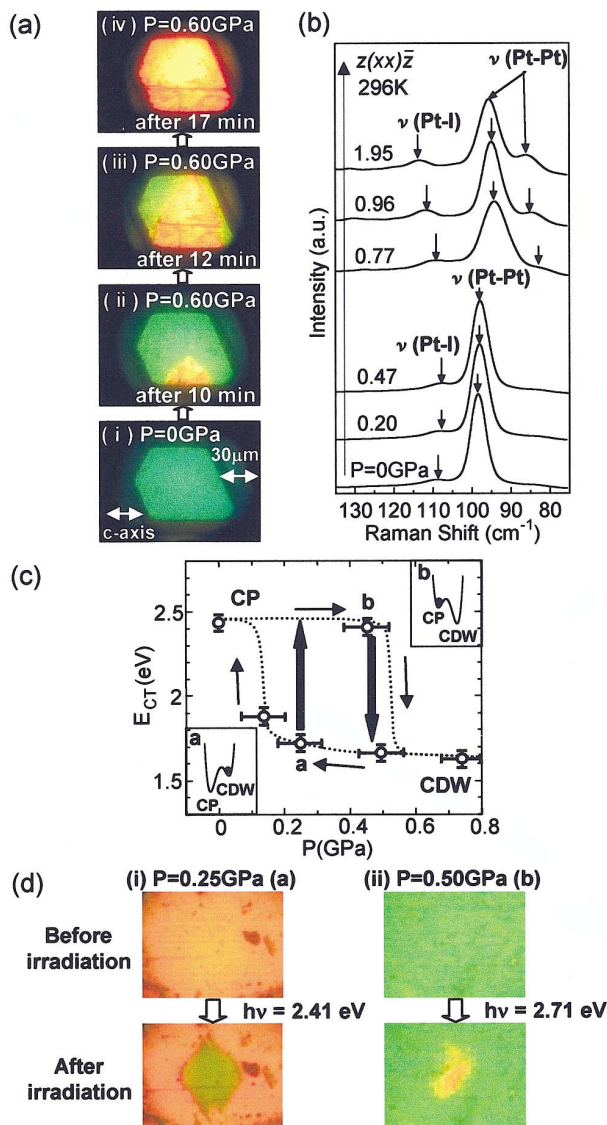


FIG. 4 (color). (a) Microscope images of $[(C_2H_5)_2NH_2]_4[Pt_2(pop)_4I]$ in the pressure-applying run. (b) Pressure dependence of Raman spectra. (c) Pressure dependence of E_{CT} . The insets show the schematic energy potential curves. (d) Microscope images at the points *a* (i) and *b* (ii) before and after photoirradiation. Polarization of the excitation light is parallel to the chain axis.

process. At *b*, PIPT could not be driven by the irradiation of 1.96-eV or 2.41-eV light, even if the intensity and duration of the light was changed. However, irradiation with 2.71-eV light for 30 s did result in a PIPT, as shown in Fig. 4(d)-(ii). As this process appears to be strongly dependent on the excitation energy, the PIPT from CP to CDW is also attributed to an optical process, although the efficiency of the PIPT from CP to CDW is much lower than that from CDW to CP.

A previous theoretical study [16] suggested that the lowest transition in CDW is an interdimer CT excitation

from $[-I-Pt^{2+}-Pt^{2+}-I-Pt^{3+}-Pt^{3+}-I-]$ to $[-I-Pt^{2+}-Pt^{3+}-I-Pt^{2+}-Pt^{3+}-I-]$. Therefore, an optical excitation in CDW will produce a local CP state. This is the reason why the CDW to CP transition is readily induced by photoirradiation. In CP, on the other hand, the intradimer CT transition from $[-I-Pt^{2+}-Pt^{3+}-I-Pt^{2+}-Pt^{3+}-I-]$ to $[-I-Pt^{3+}-Pt^{2+}-I-Pt^{2+}-Pt^{3+}-I-]$ is the dominant optical excitation corresponding to the gap transition. In this process, the CDW state is never produced, even as a local excited state. As a result, the CP to CDW transition is difficult to be achieved by the photoirradiation with the energy of 2.41 eV nearly equal to E_{CT} . As observed in the experiments, the 2.71-eV excitation drives the PIPT from CP to CDW, although the transition efficiency is very low. Such higher-energy excitation will induce the interdimer CT transition from $[-I-Pt^{2+}-Pt^{3+}-I-Pt^{2+}-Pt^{3+}-I-]$ to $[-I-Pt^{2+}-Pt^{2+}-I-Pt^{3+}-Pt^{3+}-I-]$, which may be relevant to the PIPT to CDW.

In summary, we have synthesized I-bridged binuclear Pt compounds with alkyl-ammonium and alkali metal counterions. Modulation of the interdimer distance by substitution of counterions permits the ground state to be switched between CDW and CP. The PRIPT of $[(C_2H_5)_2NH_2]_4[Pt_2(pop)_4I]$ from CP to CDW was identified, exhibiting a large hysteresis loop, and the PIPT between CDW and CP was found to be drivable within this loop. This transition behavior is an exceptional example of PIPT, demonstrating that it is possible to achieve fundamental changes in optical and magnetic properties through photoirradiation alone.

The authors thank K. Yonemitsu, M. Kuwabara, and S. Yamamoto for many enlightening discussions.

*Corresponding author.

Email address: okamoto@k.u-tokyo.ac.jp

- [1] S. Koshihara *et al.*, Phys. Rev. B **42**, 6853 (1990).
- [2] S. Koshihara *et al.*, Phys. Rev. Lett. **68**, 1148 (1992).
- [3] O. Sato *et al.*, Science **272**, 704 (1996).
- [4] M. Fiebig *et al.*, Science **280**, 1925 (1998).
- [5] Y. Ogawa *et al.*, Phys. Rev. Lett. **84**, 3181 (2000).
- [6] S. Iwai *et al.*, Phys. Rev. Lett. **88**, 057402 (2002).
- [7] M. B. Robin and P. Day, Adv. Inorg. Chem. Radiochem. **10**, 247 (1967).
- [8] M. Kuwabara and K. Yonemitsu, J. Phys. Chem. Solids **62**, 453 (2001).
- [9] S. Yamamoto, Phys. Rev. B **63**, 125124 (2001).
- [10] M. Kurmoo and R. Clark, Inorg. Chem. **24**, 4420 (1985).
- [11] N. Kimura *et al.*, Chem. Phys. Lett. **220**, 40 (1994).
- [12] C. Bellitto *et al.*, Inorg. Chem. **22**, 444 (1983).
- [13] H. Kitagawa *et al.*, J. Am. Chem. Soc. **121**, 10 068 (1999).
- [14] D. Baeriswyl and A. R. Bishop, J. Phys. C **21**, 339 (1988).
- [15] C.-M. Che *et al.*, J. Am. Chem. Soc. **105**, 4604 (1983).
- [16] M. Kuwabara and K. Yonemitsu, J. Mater. Chem. **11**, 2163 (2001).